Environmental Research 208 (2022) 112741

Contents lists available at ScienceDirect

Environmental Research

journal homepage: www.elsevier.com/locate/envres

Nanoplastics measurements in Northern and Southern polar ice

Dušan Materić [a,*], Helle Astrid Kjær [b], Paul Vallelonga [b], Jean-Louis Tison [c], Thomas Röckmann [a], Rupert Holzinger [a]

[a] Institute for Marine and Atmospheric Research Utrecht, Utrecht University, Princetonplein 5, 3584CC, Utrecht, the Netherlands
[b] Section for the Physics of Ice, Climate and Earth, The Niels Bohr Institute, University of Copenhagen, Copenhagen, Denmark
[c] Laboratoire de Glaciologie, DGES-IGEOS, Université Libre de Bruxelles, Brussels, 1050, Bruxelles, Belgium

ARTICLE INFO

Keywords:
Nanoplastics
Microplastics
PTR-MS
Polar regions
Greenland
Antarctic

ABSTRACT

It has been established that various anthropogenic contaminants have already reached all the world's pristine locations, including the polar regions. While some of those contaminants, such as lead and soot, are decreasing in the environment, thanks to international regulations, other novel contaminants emerge. Plastic pollution has been shown as a durable novel pollutant, and, since recently, smaller and smaller plastics particles have been identified in various environments (air, water and soil). Considerable research already exists measuring the plastics in the 5 mm to micrometre size range (microplastics). However, far less is known about the plastics debris that fragmented to the sub-micrometre size (nanoplastics). As these small particles are light, it is expected that they have already reached the most remote places on Earth, e.g. transported across the globe by air movement. In this work, we used a novel method based on Thermal Desorption – Proton Transfer Reaction – Mass Spectrometry (TD-PTR-MS) to detect and measure nanoplastics of different types in the water sampled from a Greenland firn core (T2015-A5) and a sea ice core from Antarctica. We identify polyethylene (PE), polypropylene (PP), polyethylene terephthalate (PET), polystyrene (PS), polyvinyl chloride (PVC), and Tire wear nanoparticles in the 14 m deep Greenland firn core and PE, PP and PET in sea ice from Antarctica. Nanoplastics mass concentrations were on average 13.2 ng/mL for Greenland firn samples and 52.3 ng/mL for Antarctic sea ice. We further discuss the possible sources of nanoplastics that we found at these remote locations, which likely involve complex processes of plastic circulation (emission from both land and sea surface, atmospheric and marine circulation).

1. Introduction

It has recently been discovered that novel anthropogenic pollution which originate from fossil fuel polymer production are present in the air, water and soil. Polymers such as plastics have been commonly used since the middle of the last century with increasing yearly production that in 2019 reached 368 million tonnes worldwide (Geyer et al., 2017; PlasticsEurope, 2019, 2021). Such a massive production of durable polymers results in a littering problem. Polymers that are disposed of in the environment fragment to microplastics (1 μm–5 mm size) and nanoplastics (particles size <1 μm) (Bianco et al., 2020; Bond et al., 2018; Dawson et al., 2018; Geyer et al., 2017; Napper and Thompson, 2019; Vicente et al., 2009). Mismanaged plastics enter soils and rivers, have been delivered to the world's oceans (González-Fernández et al., 2021; Lebreton et al., 2017; Liss, 2020; Wayman and Niemann, 2021; Weiss et al., 2021), and transported to remote places (Allen et al., 2019; Brahney et al., 2020; Materić et al., 2021b; Zhang et al., 2021). Most of the research and plastic inventories assessments have focussed on a fairly large size fraction of plastics – micro and macroplastics (pieces >5 mm), while nanoplastics have escaped attention because they are not detectable by the standard sampling and measuring protocols (Lindeque et al., 2020; Poulain et al., 2019; Wayman and Niemann, 2021).

Large unknowns also exist in our present-day understanding of the global scale circulation of plastics through our environment. While the transport of microplastics between terrestrial and marine areas is to some degree understood (Allen et al., 2020; Brahney et al., 2021; Evangeliou et al., 2020), far less is known about the nanoplastics. Nanoplastics seem to compose a significant proportion of the plastics debris budget. Several methodological approaches, both quantitative and semi-quantitative, indicated the presence of nanoplastics in environmental samples of seawater (North Atlantic, Dutch Warden Sea), rivers (the UK), regional and remote surface waters (Sweden and

* Corresponding author.
E-mail address: d.materic@uu.nl (D. Materić).

https://doi.org/10.1016/j.envres.2022.112741
Received 26 November 2021; Received in revised form 11 January 2022; Accepted 12 January 2022
Available online 19 January 2022

Siberia, Russia) and snow in the remote high-altitude Alps (Austria) (Davranche et al., 2020; Materić et al., 2020, 2021a, 2021c; Sullivan et al., 2020; Wahl et al., 2021; Xu et al., 2020). These first measurements of environmental nanoplastics already suggest the omnipresence of nanoplastics. They confirm the hypothesis that nanoplastics *do* form in the environment and *can* be transported to locations far away from the original sources.

Natural, environmental erosion of bigger plastic materials may form the nanoplastics in various ways that involve physical, chemical and biological processes (Dawson et al., 2018; El Hadri et al., 2020; Napper and Thompson, 2019). As these small particles are light, they have a potential to get airborne and deposited in urban, rural and remote areas. They are also good candidates for reemission from secondary sources such as urban surfaces and agricultural soil (Brahney et al., 2021; Rezaei et al., 2019; Tagg et al., 2021). However more measurements are needed to understand the magnitude of all the processes involved including sources, sinks and transport of nanoplastics.

In this work, we went to the most remote places on Earth, beyond the South and North polar circle, in search of nanoplastics in polar ice. We analysed samples from a 14 m deep firn core from central Greenland and from a sea ice core from Antarctica. Our goal was to demonstrate the presence of nanoplastics in these remote areas, to characterize them and to give a first insight into possible processes involved in their transport.

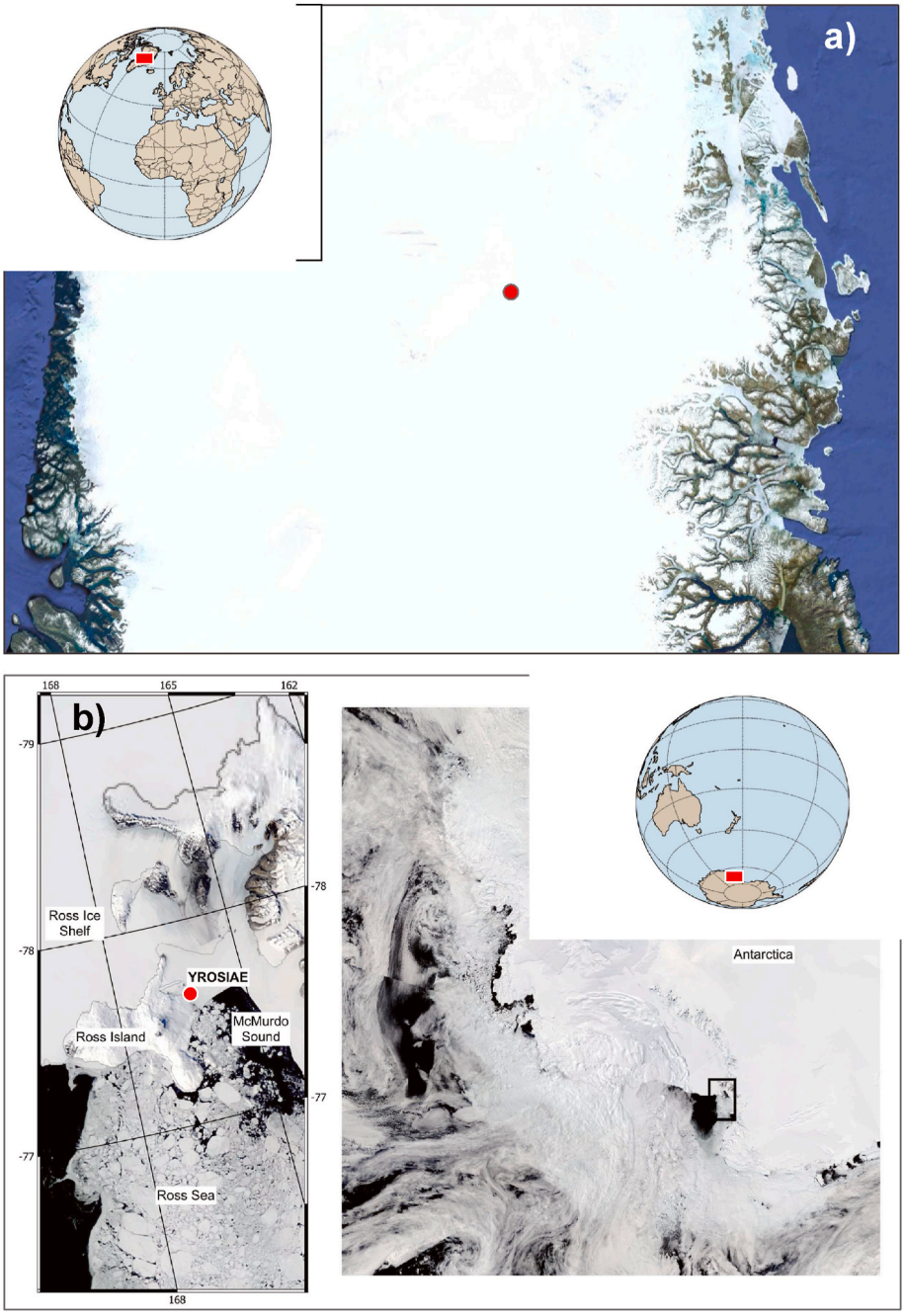

Fig. 1. Location of the study sites: a) Greenland −75N37.501′, 35W58.809′ close to the EastGRIP deep drilling site; b) Antarctica − Cape Evans 77°38′S, 166°23′E in McMurdo Sound (adapted from Van der Linden et al., 2020). The sampling locations are presented as red dots. (For interpretation of the references to colour in this figure legend, the reader is referred to the Web version of this article.)

2. Material and methods

2.1. Sampling of the shallow firn core, Greenland

During a traverse from NEEM (North Greenland Eemian Ice Drilling Project) to EastGRIP (East Greenland Ice core Project - Kjær et al., 2021a, 2021b) in 2015 a shallow firn core (T2015-A5) was collected at 75N37.501′, 35W58.809′ down to 14.02 m close to the EastGRIP deep drilling site (Fig. 1a).

The firn core was drilled using the U.S. Ice Drilling and Design Operations hand auger (76 mm diameter). In the field, the cores were split into 55 cm long segments and packed into plastic bags made from polyethylene (PE). They were then stored in cooler boxes made from expanded polypropylene (PP) and transported on sledges to the EastGRIP site, from where they were flown first to Kangerlussuaq, Greenland, and then shipped further to Copenhagen, Denmark for storage and analysis. In Copenhagen, the cores were stored at −20 °C until further cutting into sections of 3.4 × 3.4 cm just prior to measurements by Continuous Flow Analysis (CFA) at the Niels Bohr Institute (Bigler et al., 2011).

Continuous flow analysis is a common method for analysing ice cores and for the Copenhagen CFA system, as presented by Bigler et al. (2011), determines conductivity (σ), insoluble dust, ammonium (NH_4^+) and calcium (Ca^{2+}). The system was slightly adjusted (Kjær et al., 2016) so that hydrogen peroxide (H_2O_2) and acidity were also analysed on the firn core T2015-A5. Details of the CFA setup and instrumentation is presented in (Kjær et al., 2021b). Based on annual layer counting of H_2O_2 summer peaks and insoluble dust/calcium winter peaks, we observed a mean annual accumulation of 14.6 ± 3.1 cm w.eq and date the bottom of the firn core T2015-A5 back to ~1966.

2.2. Subsampling and melting of firn for nanoplastics analysis

During the melting and continuous flow analysis, one meltwater line was devoted for subsampling for the TD-PTR-MS analysis. Discrete samples were collected every 27.5 cm of the core (two samples per 55 cm segment). Great care was taken that only the inside part of the core was sampled, thus, our sample never had contact with the field or lab atmosphere, packing material, or sampling equipment. However, it had contact with the melting head and the pipes of the CFA system. Between the melting of the core sections, we melted and subsampled the blanks. The blanks for this analysis were made by freezing Milli-Q water in plastic bags similar to the ones used for transport of the firn cores from the field, and cut into 3.4 × 3.4 cm sections. Such ice blanks were melted in-between the continuous firn sample melting and thus represent the blanks for the entire CFA system, including the cutting in the freezer and the exposure to the plastic bags (PE) used for transport. In other words, these complete process blanks were exposed to all the impurities the core was exposed to. As the relevant inner part of the cores were not directly exposed to contamination at any moment in the field, core transport or storing, no field blanks (e.g. Milli-Q water exposed to the air of the site) were taken. After the melting at the CFA system, the samples and complete process blanks were stored in dark and cold (4 °C) in PP vials.

2.3. Antarctic sea ice core sampling and ancillary measurements

The sea ice core sampling took place at Cape Evans (77°38′ S, 166°23′E), located on the eastern side of McMurdo Sound, under the western slopes of Mt Erebus, Ross Island, Antarctica (Fig. 1b), in the framework of the YROSIAE (Year-Round Ocean-Sea Ice Atmosphere Exchanges) Belgian project. A smooth and flat fast sea ice cover develops each year under quiescent conditions and typically reaches thicknesses between 1.5 and 2.5 m. Sampling occurred in two phases: from 28 November to December 8, 2011, and from 19 September to November 1, 2012 (see Carnat et al., 2014 for a full description). During the first phase, an ice coring site was delineated with flags approximately 400 m away from the shore. The exact same location was re-visited during the second phase but, obviously, with a renewed sea ice cover.

The sea ice coring site was visited three times during phase 1 and five times during phase 2. We show here measurements performed on ice collected during the sampling event of October 17th, 2012 (YROSIAE Station 6) of phase 2. Each time the site was visited, a small sampling square area (10 m^2) was delineated. Sampling always started with a basic description of the snow cover. Ice cores were then taken using an electropolished stainless-steel ice corer (14 cm ID). Ice cores were immediately wrapped in polyethylene bags and kept at < −30 °C, horizontally in the dark to prevent brine drainage from the cores (Cox and Weeks, 1986) and limit the physiological activity of ice algae. In the field, this was achieved by placing the cores in an insulated box prefilled with cold packs frozen at −30 °C.

All the physical properties of the sea ice cover were assessed on a dedicated ice core. The first half of the core was used to determine the *ice texture*. Thick vertical sections of the core were cut with a bandsaw and attached to glass plates by freezing Milli-Q water along the edges of the sections. The thick sections were planed down to thin sections of 600–700 μm using a Leica® SM2400 microtome. These thin sections were then installed on a light table equipped with cross-polarized sheets (Langway, 1958). Ice types were identified based on visual observation of the size, shape, and orientation of the ice crystals, and compared to descriptions found in the literature (Eicken and Lange, 1989; Tison et al., 1998).

Ice temperature was measured on site on the second half of the core dedicated to physical properties, using a fast response handheld portable digital thermometer equipped with a TESTO®720 calibrated probe (precision ±0.1 °C, accuracy ±0.2 °C). The probe was inserted in 2 mm diameter holes freshly drilled along the core every 5 cm.

Bulk ice salinity was measured using the same vertical resolution as for ice temperature. In the cold room, the half core was bisected down the middle and sectioned (5 cm increments) using a stainless-steel band saw. The sections were then allowed to melt at room temperature in sealed plastic containers, a process taking approximately 12 h. Bulk salinity was determined through conductivity by inserting the probe of a Thermo-Orion® WP-84 TPS meter in each melted ice section (accuracy of ±0.1‰). Finally, the *brine volume fraction* (proportion of salty liquid inclusions entrapped in the ice as pockets, intracrystalline layers or brine channels) was calculated from temperature and bulk ice salinity, using the formulation recommended by Petrich and Eicken (2017).

2.4. Subsampling and melting of sea ice for nanoplastics analysis

The top and bottom part of the sea ice core was cut with a clean stainless-steel blade, so the surfaces were for the first time exposed during this process. Such samples were placed in a new clean glass jar. The samples were cut immediately before the analysis and were melted for the first time just before the TD-PTR-MS analysis.

2.5. Analysis by TD-PTR-MS

The analysis was performed as previously described in Materić et al., (2020). In short, 1.5 mL of melted ice samples (and blanks, ultrapure HPLC water, VWR Chemicals) were filtered through a 200 nm membrane syringe filter (UNIFLO 25/0.2 PT FE) to separate microplastics from nanoplastics. Filtered water was loaded as 1.5 mL aliquots and processed by low-pressure evaporation/sublimation as described in our previous work (Materić et al., 2017, 2020). After the water had been removed, we performed thermal desorption of the remaining material starting from 35 °C and ramping to 350 °C at the rate of 40° per minute, keeping at 350 °C for 5 min. During the thermal desorption, we continuously (every second) monitored the organic ions signals with a PTR-TOF-MS (PTR8000, IONICON Analytik, AU), using previously described settings (E/N 120 Td) (Materić et al., 2017, 2020).

The procedural blanks were treated the same as the sample. The same filtering procedure, labware and processing was used for the procedural blanks (more on the blanks and contamination assessment in the Quality control section). Samples were analysed in triplicates.

2.6. Data processing and evaluation

Raw mass spectra were analysed first using PTRwid (Holzinger, 2015), where the measured mole fractions were exported for each ion of the mass spectra. The signal for each ion was integrated for 8 min (7 min for sea ice samples) starting when the temperature of the thermal desorption oven reached 50 °C. This resulted in one mass spectrum per TD run.

The ion signal of samples was corrected for the mean signal of the blanks from HPLC water for sea ice samples and system blanks (clean vials) for Greenland samples, and a 3-sigma detection limit was applied. The blank correction and detection limit filter were applied to all the replicates.

The final mass spectra were used for nanoplastics fingerprinting, as explained in our previous work (Materić et al., 2020, 2021b). In short, the mole fraction ratios of 40 ions from virgin plastics were compared to the same ions measured in the environmental samples. The similarity between plastics and sample ions was compared, scored and evaluated. The threshold score that defined a positive match was calculated based on 1000 random/synthetic mass spectra, which included the same 40 ions as in the library mass spectra. If the signal was 2σ above the average of the synthetic spectra (z-score = 2, $p < 0.02275$, one tail distribution), we assigned a positive fingerprint for that particular plastic type (for more details, see Materić et al., 2021b). The similarity in mass spectra between pure plastics standards (PET and PE) and ice samples are shown in Fig. 2.

When the fingerprint score was positive, each organic ion typical for the matched plastics type was quantified in the environmental samples according to the standard PTR-MS formula (Cappellin et al., 2012; Holzinger et al., 2019; Lindinger et al., 1998; Materić et al., 2017; Peacock et al., 2018):

$$[mf] = \frac{1}{kt} \times \frac{[M{\cdot}H^+]}{[H_3O^+]} \times \frac{\sqrt{(m/z)_{H_3O^+}}}{\sqrt{(m/z)_{M{\cdot}H^+}}}$$

where [*mf*] is mole fraction in ppb, *k* is reaction rate coefficient, *t* the residence time of the primary ions in the drift tube, $[M{\cdot}H^+]$ and $[H_3O^+]$ are ion counts representing the protonated analyte and primary ions, respectively, $(m/z)_{H3O+}$ and $(m/z)_{M{\cdot}H+}$ represent the mass-to-charge ratio of protonated water and the protonated analyte *M,* respectively, which corrects for the TOF duty cycle. Mole fractions are further converted to the final concentrations (ng/mL), considering dilution of the airstream and the volume of the samples loaded, preserving the ratio of ion intensities as in the mass spectrum of the virgin plastics – thus correcting for the overestimation as explained in Materić et al. (2020). All the data processing stages including the raw data files are available in the Supplementary Data (see the Appendix).

The final concentrations we present in this work are the amounts of plastic vapours successfully ionised in the TD-PTR-MS system. As the ionisation efficiency is not 100% (e.g. some organic ion-fragments and CO_2 do not ionise in the system), these results (±60% uncertainty, see quality control section) should be considered semi-quantitative, and as such, they represent low threshold values of the actual concentrations in the environmental samples (Materić et al., 2020, 2021b). Unfortunately, at the moment, the ionisation efficiencies for different plastic polymers cannot be experimentally deduced (apart from PS) due to the lack of analytical standards for nanoplastics (Holzinger et al., 2019; Materić et al., 2020).

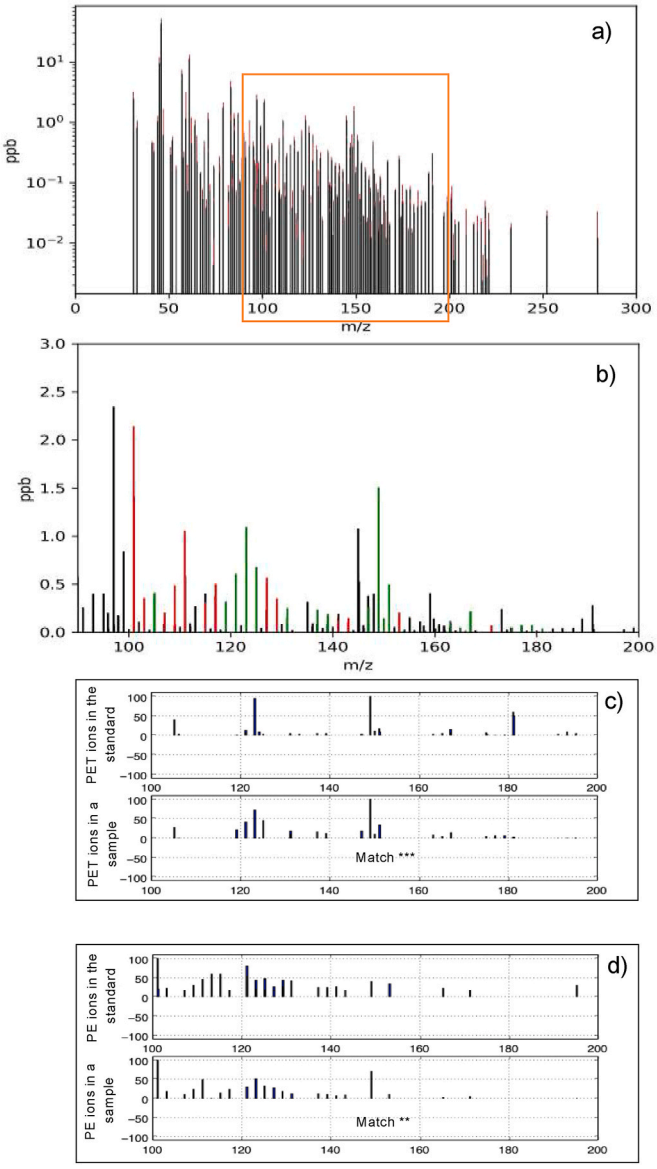

Fig. 2. PTR-MS mass spectra for plastic standards and sea ice samples from the Antarctic (bottom part of the core). a) mass spectrum of the Antarctica sea ice, standard deviation of replicas are shown in red, note that the y-axis has a logarithmic scale; b) zoomed-in mass spectra with plastics fingerprinting ions shown in colour (PE red, PET green); c) normalised mass spectra for PET standard and the sea ice sample – match confidence "***" >4σ ($p < 000032$); d) normalised mass spectra for PE standard and the sea ice sample – match confidence "**" >3σ ($p < 0.00135$). Note the similarity between organic ion profiles of the virgin plastic standards and the sea ice samples (panels c and d). (For interpretation of the references to colour in this figure legend, the reader is referred to the Web version of this article.)

2.7. Quality control

During our sampling and analyses, it was impossible to avoid the use of plastic polymers. For example, both ice cores (Greenland and Antarctica) were initially stored in a polymer material of certain types (PE, PP). However, those plastics only touched the surface of the cores. So, the inside part of the cores was not in contact with a plastics polymer, and it was all the time shielded from air exposure by at least 1.4 cm of ice. The Greenland ice core was melted in the continuous melting system so that only the inside, most pristine, part of the core was sampled for TD-PTR-MS analysis. The Antarctic sea ice core was cut before analysis, and only the inside part of the core was used, which had not been in

contact with plastic material or directly exposed to the air before cutting. That way, we avoided/minimised the possibility of the plastic materials and dust particles touching our samples and contaminating them during processing.

For assessing possible contamination during the sampling and sample handling, we performed different blank measurements. We analysed clean vials as the system blanks, Milli-Q water or HPLC water as process blanks, and frozen Milli-Q ice that was melted and run through the entire automated melting process as the Greenland ice core (complete process blanks).

Some plastics materials were used for handling samples and process blanks, such as syringes (PE, rubber stopper), membrane filters (PE, PTFE) pipet tips (PP). However, all our process blanks were exposed to the same impurities (filtered with the same kit, the same labware used). Our process blanks were assessed for plastic traces, and no plastic contamination on any plastic types analysed here has been found in any of the blanks (see the supplement for the mass spectra and fingerprint scores). To our best knowlage, nanoplastics contamination does not happen much from new, high-quality labware, but rather from exposure of the samples/blanks to the air. Thus, we minimised the air exposure of the samples at all times.

The downside of the TD-PTR-MS method we used in this work is that we cannot provide the size distribution of the nanoplastic particles, neither their shapes or colour. Furthermore, due to the mass spectra similarity, it is not possible with the current fingerprint method to differentiate PP from PPC (polypropylene carbonate), or to resolve PE of different densities. There is also some similarity between mass spectra of PP and PE. For example the fingerprint method used in this work, "Algorithm 1" and "Algorithm 3" (Materić et al., 2020), which are the most conservative routines, show a weak false positive fingerprint (match score "*") when a PP standard is compared against virgin PE, but not the other way round (see SD). This means that the relative contribution of PE might be underestimated at the expense of PP. Thus, the reported PE loads are on the conservative side (no PE false positive in PP), however, 0–58% of semi-quantitative PP loads reported in this work might be PE nanoplastics (see SD for the calculation). It is important to note, though, that the PP fingerprint for many of our ice samples had a stronger match score (e.g. "**" or "***", see caption Figure A1 and Fig. 2, all scores available in SD) compared to the false positive match score between pure PP and PE, which suggests that PP is indeed present in our samples (see Figure A1).

The ion similarity of the mass spectra for different plastics types (even one that did not pass the threshold of fingerprint detection) could contribute to the ion signal in a sample. Considering all the limitations (e.g. mass spectra similarity between different plastic types, PTR-MS standard quantification error), we estimate an uncertainty of ±60% for the reported semi-quantitative results.

3. Results and discussion

3.1. Greenland

The average concentration of the nanoplastics found in the Greenland ice core was 13.2 ng/mL. Different plastics types were detected with mean concentrations for PE 6.5 ng/mL, PET 2.7 ng/mL, PS 0.11 ng/mL, PVC 0.11, PP/PPC 0.57 ng/mL and Tire wear 3.2 ng/mL. Other data measured on the CFA system for the core, averaged to the same sampling resolution of the plastics analysis are available in SD (see the Appendix).

PE was the dominant plastics type in the Greenland firn core (Fig. 3) and contributed 49% to the total nanoplastics mass. PE is one of the most used types of plastic, common in single-used packing materials (disposable bags and food containers), houseware, pipes and agricultural foils (PlasticsEurope, 2019). PE demand in Europe in 2019 was more than 14 million tonnes and accounted for 29.8% of all plastics used (PlasticsEurope, 2021). Earlier work shows that PE is one of the most common microplastic types found in the Greenland subsurface seawater, Arctic snow, and surface sea water of the North sea (Bergmann et al., 2019; Lorenz et al., 2019; Morgana et al., 2018), which is consistent with our results. PE nanoplastics may come from multiple sources to this remote site: 1) from land via atmospheric long-range transport (Legrand et al., 2016; Schüpbach et al., 2018) or 2) from the sea surface (Allen et al., 2020), where PE macro- and microplastics fragment to nanoplastics via e.g. UV degradation (Wayman and Niemann, 2021), which airborne via bubble burst process (Masry et al., 2021) and finally deposit at the sampling site.

The next most important nanoplastic types at the Greenland site were PET and Tire, with respective relative contribution of 21 and 24%. PET fibres are associated with the clothes and clothing industry (Chan et al., 2021; Liu et al., 2021). It is also extensively used in bottle productions (e.g. for water and soft drinks), and the European demand for such use in 2019 was ca. 4 million tonnes (PlasticsEurope, 2021). PET is one of the dominant forms of microplastic fibres in the urban atmosphere (Cai et al., 2017; Dris et al., 2016; Zhu et al., 2021). The wind trajectories for the sampling site in Greenland have been previously modelled, and point to long-range transport from North America and Asia (Legrand et al., 2016). Previous research showed that PET microplastics had been transported via air and sea currents to remote North Arctic sites, and it has been measured in seawater, snow and ice (Bergmann et al., 2019; Morgana et al., 2018; Ross et al., 2021). On the continent, PET microplastics have been identified in many remote locations and the transport modelling indicates urban areas as dominant sources (Allen et al., 2019; Bergmann et al., 2019; Evangeliou et al., 2020; Zhang et al., 2021). Less is however known so far for nanoplastics transport. PET nanoplastics deposition has been only measured in the remote high-altitude Alps where back trajectory analysis points to urban, populated areas in western Europe as main source (Materić et al., 2021b).

Thus, the origin of nanoplastics at this Greenland site is likely a

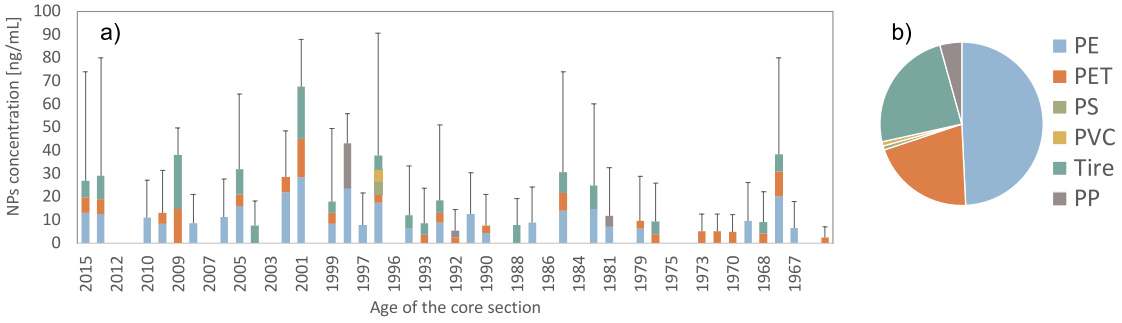

Fig. 3. Nanoplastics concentrations at different depths of our Greenland's firn-core (T2015-A5) sampled at 27.5 cm length resolution. a) Polymer type contribution for each sampling depth. The error bars represent the standard deviation of the replicas. B) average contribution of each polymer type in the analysed samples.

combination of different transport processes involving sea and air transport. Recent increase in visits (tourism, expeditions) might also be a contributor for the most recent ice sections. Nanoplastics found here may be deposited from primary sources (e.g. urban places, agricultural fields, mismanaged waste sites) or originate from secondary sources (e.g. microplastics that have previously been deposited far away from the original sources and recirculate in the environment – e.g. sea surface, roads) (Brahney et al., 2021; Evangeliou et al., 2020).

3.2. Antarctica

For the Antarctic sea ice samples, the average nanoplastics concentration at the top and bottom were 67.0 and 37.7 ng/mL, respectively (Fig. 4). The relative contribution of the different plastic types is also shown in Fig. 4. PE is the most abundant type of nanoplastics in this Antarctic sea ice core, contributing more the 50% by mass (38.0 and 19.8 ng/mL for the top and bottom of the core, respectively). The second most common type of nanoplastic measured at this site was PP with a concentration of 20.7 ng/mL at the top and 9.0 ng/mL at the bottom (relative contribution of 31 and 24%, for the top and the bottom part of the core, respectively). While the PE and PP nanoplastics concentration is higher in the top layer of the sea ice core, the mass of PET seems similar at the top and bottom of the core, 8.3 and 8.9 ng/mL, respectively. No Tire-generated nanoplastics were detected in our Antarctic sea ice samples.

It has been previously reported that the dominant types of microplastics in the Ross Sea and Antarctica sea ice are PE and PP, which agrees with our results for nanoplastics (Cincinelli et al., 2017; Kelly et al., 2020). Unlike these previous works, which showed the presence of little or no PET microplastics in Antarctica, we found a noticeable contribution of PET nanoplastics in the sea ice.

We have not observed PS nanoplastics, although some research indicated PS microplastics presence in the ice and atmosphere from Antarctica (González-Pleiter et al., 2021; Marina-Montes et al., 2022). The absence of PS nanoplastics in our sample could be explained by the processes at work during the sea ice formation. Impurities show contrasting behaviour regarding initial incorporation at the growing sea ice interface: some show conservative behaviour with respect to sea water salinity, others are decoupled due to biological processes (e.g. NO_3, SiO_2, dissolved and particulate Fe, O_2, CO_2, CH_4) transport processes within the brine inclusions (e.g. gas bubbles) or interactions with biogenic biofilms (e.g. EPS; $CaCO_3$, NO_3^-, dissolved and particulate Fe). Very little is known for nanoplastics. A recent study from Alice et al. (2021) suggests that large PS particles, such as microplastics, are selectively incorporated into the sea ice, while nanoplastics are expulsed from it and stay in the water below. An experimental study from Geilfus et al. (2019) showed that indeed the surface sea ice layers (few centimetres) are enriched in larger microplastics (>1000 μm), due to the low density of the microplastics concentrating them at the sea water surface and to the initial frazil ice scavenging. However, as the sea ice grows, much less microplastics are incorporated, and the larger sizes become less abundant (in relative %) than in the original water, while the smaller microplastics fraction (125-63 μm) increases and reaches higher relative % than in the original water.

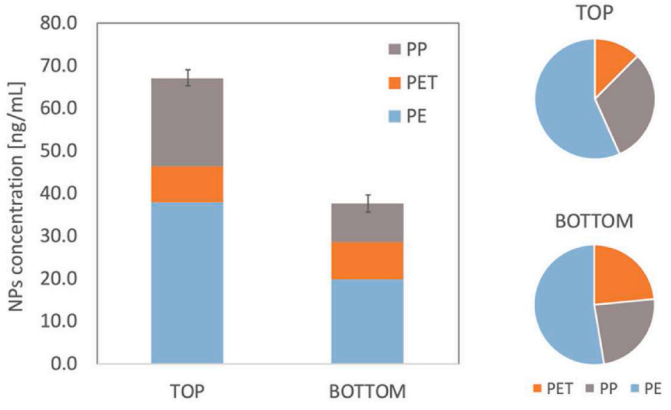

Fig. 4. Nanoplastics concentration and types at top and bottom of the YROSIAE Station 6 sea ice core. The error bars represent the standard deviation of the triplicates.

The sea ice samples used in this study are from Antarctic landfast sea ice (attached to the "land", be it rock or floating ice), as opposed to pack ice that freely drifts in the open ocean. Its crystal structure (ice types in Fig. 5a) is typical of the area: a thin layer of frazil ice at the very top, which forms from the aggregation of individual ice crystals formed in the turbulent surface water as the temperatures drop down, and the sea ice cover starts to form. The texture quickly switches to vertically elongated columnar ice crystals, with the transition to a quiet growth regime under the initially consolidated frazil. Then, more specific of the landfast sea ice forming in front of ice shelves, the facies changes to platelet ice. These are crystals forming in supercooled water emerging at the front of the ice shelf (in a water mass known as Ice Shelf Water that originates under the several 100 m-thick floating ice shelf, further towards the continent-see Hoppmann et al., 2020 for a review) and accreting under the sea ice cover, usually starting mid-July in the McMurdo Sound area.

The physical properties of the sea ice cover are summarized in Fig. 5. The temperature profile is sub-linear (Fig. 5c), indicating near-equilibrium between the ocean melting point temperature at the bottom and the still quite cold temperatures at the ice surface at this end of the winter period. The brine volume (Fig. 5e) is therefore quite low, and apart from the bottom 25 cm, below the critical value of 5%, which is considered as the threshold for impermeable ice (with sufficiently low temperatures at a given bulk ice salinity, the brine inclusions split into disconnected pockets) (Golden et al., 1998). The bulk ice salinity profile (Fig. 5d) hovers between 13 and 4, witnessing the generalized rejection of salts from the sea ice as it grows in 35 salinity sea water. It is typically "C-shaped" (Petrich and Eicken, 2017), with higher salinities at the top due to less efficient rejection in fast-growing ice and at the bottom due to the higher brine volume content in this warmer, slowly growing ice (thermodynamic equilibrium between ice and brine).

Regarding the potential source of nanoplastics at this location, several observations can be made. In terms of sea ice incorporation

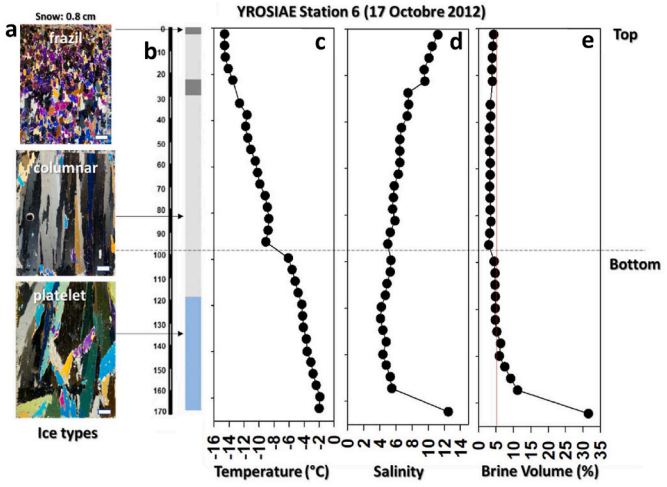

Fig. 5. Summary of the basic physical properties of the sea ice cover at Station YROSIAE 6, sampled on October 17th, 2012: a) example of ice types, b) continuous ice types vs. depth (cm), c) ice temperature, d) bulk ice salinity and e) Brine volume (%). The stippled horizontal line shows the limit between Top and Bottom of the ice core that have been used for the nanoplastics concentration measurements (modified from Carnat et al., 2014).

processes, a direct pathway from the atmosphere to the sea ice surface is probably limited, since a) there is very little snow deposition (less than 1 cm for the whole season in this area) and b) most of the ice is impermeable, prohibiting the downward transfer of surface contamination throughout the brine channel network. Dry deposition at the surface of the ice however remains an option for the top sample. Local anthropic contamination is not excluded here (especially for top part of the core) but it is unlikely as the sampling site is located ~22 km away from the US McMurdo Station.

Surface sea water is therefore probably the dominant source for incorporation into the sea ice. The decrease from top to bottom of the nanoplastics concentration by a factor of 2, similar to what is observed with the bulk ice salinity, might indicate a "passive" conservative tracer behaviour during incorporation into the sea ice.

However, a more likely explanation for the top/bottom contrast in our sea ice core might be found in the origin of the water freezing into sea ice: In the first part of the season, it is mainly the surface open water that freezes to form granular and then columnar ice. From July onwards, the accretion of platelet ice in supercooled water originating from deep below the ice shelf, therefore more protected from surficial sources of plastics, might explain the concentration drop. Polar sea currents which indicate the origin of such water in the context of microplastics are modelled and described elsewhere (Rowlands et al., 2021).

3.3. Implications

To our knowledge, this is the first work that quantifies nanoplastics concentration in the polar region (with low thresholds of the concentrations). Although the magnitude of nanoplastics impact on the environment is still not completely understood, this work provides one of the first empirical data for environmental nanoplastics loads in remote areas.

Nanoplastics have shown various adverse effects on organisms exposed to it. For marine organisms, nanoplastics can have a toxic effect, affecting the growth, inducing delayed development, generating larval malformation and subcellular changes such as increased reactive oxygenated species (ROS) levels and lysosomal destabilization (Ferreira et al., 2019; Lehner et al., 2019). Human exposure to nanoplastics can result in cytotoxicity, inflammation, and ROS production (Lehner et al., 2019).

On the other hand, small plastics particles in the atmosphere can scatter and absorb the light, thus influencing Earth's effective radiative forcing by up to -0.75 mW/m^2 (Revell et al., 2021). Effects of micro and nanoplastics particles in clouds (e.g. cloud condensation nuclei) and when deposited at the snow/ice surfaces in the context of Earth's albedo, are not yet known, primarily due to the lack of empirical data. More research is clearly needed to focus on measuring environmental nanoplastics so that the risk of "ecological surprise" can be timely minimised (Baho et al. n.d.).

4. Conclusions

In this work, we measured nanoplastics composition in samples from a 14 m Greenland firn core and a sea ice core from Antarctica. Nanoplastics mass concentrations were on average 13.2 ng/mL for Greenland and 52.3 ng/mL for sea ice from Antarctica. In both Southern and Northern polar samples, PE was the dominant nanoplastic type contributing ~50% by mass, which agrees with the previous findings for microplastics from similar sites. The transport pathways of nanoplastics that reached these remote North and South polar locations likely involve a combination of complex processes including both atmospheric and marine transport, (re)emission, deposition and ice incorporation. Further studies are clearly needed to constrain better the source of theses contaminants to the polar regions.

Author contributions

DM conceived the paper. PV and HAK organized sampling and provided samples from Greenland. DM, HAK and PV melted the snow firn to sample for TD-PTR-MS. JLT planned and carried out the sampling in Antarctica. DM performed TD-PTR-MS analysis, wrote the manuscript with ideas and feedback from all co-authors.

Data and materials availability

All data needed to evaluate the conclusions in the paper are present in the paper and in the Supplementary Information (including raw files, all the scripts and processing stages of the data analysis) and it is available in the YODA public repository:https://doi.org/10.24416/UU01-H8ZO62.

Declaration of competing interest

The authors declare that they have no known competing financial interests or personal relationships that could have appeared to influence the work reported in this paper.

Acknowledgements

DM and RH acknowledge support from Dutch Research Council (Nederlandse Organisatie voor Wetenschappelijk Onderzoek – NWO) project "Nanoplastics: hormone-mimicking and inflammatory responses?" (grant number OCENW.XS2.078), and project "Plastic Air" (grant number OCENW.XS.066). DM, RH and TR acknowledge support from Dutch Research Council The Netherlands Earth System Science Centre (NESSC) research network (grant number 024.002.001).

EGRIP is directed and organized by the Centre for Ice and Climate at the Niels Bohr Institute, University of Copenhagen. It is supported by funding agencies and institutions in Denmark (A. P. Møller Foundation, University of Copenhagen), USA (US National Science Foundation, Office of Polar Programs), Germany (Alfred Wegener Institute, Helmholtz Centre for Polar and Marine Research), Japan (National Institute of Polar Research and Arctic Challenge for Sustainability), Norway (University of Bergen and Trond Mohn Foundation), Switzerland (Swiss National Science Foundation), France (French Polar Institute Paul-Emile Victor, Institute for Geosciences and Environmental research), Canada (University of Manitoba) and China (Chinese Academy of Sciences and Beijing Normal University).

The YROSIAE sea ice Project was supported by the Belgian FRS-FNRS (project YROSIAE, contract 2.4517.11), Belgian Science Policy (project BIGSOUTH, contract SD/CA/05), Antarctica New Zealand (project K131) and the Canada's National Science and Engineering Research Council (NSERC).

The authors thank Dr C. Sapart and Dr. C. Jacques for their contribution in re-sampling the sea ice cores at Utrecht University.

Appendix A. Supplementary data

Supplementary data to this article can be found online at https://doi.org/10.1016/j.envres.2022.112741.

References

Alice, P., Maud, G., Dominique, B., Julien, G., 2021. Micro- and nanoplastic transfer in freezing saltwater: implications for their fate in polar waters. Environ. Sci.: Processes Impacts. https://doi.org/10.1039/D1EM00280E.

Allen, S., Allen, D., Moss, K., Roux, G.L., Phoenix, V.R., Sonke, J.E., 2020. Examination of the ocean as a source for atmospheric microplastics. PLoS One 15, e0232746. https://doi.org/10.1371/journal.pone.0232746.

Allen, S., Allen, D., Phoenix, V.R., Roux, G.L., Jiménez, P.D., Simonneau, A., Binet, S., Galop, D., 2019. Atmospheric transport and deposition of microplastics in a remote mountain catchment. Nat. Geosci. 1 https://doi.org/10.1038/s41561-019-0335-5.

Baho, D.L., Bundschuh, M., Futter, M.N, n.d. Microplastics in terrestrial ecosystems: moving beyond the state of the art to minimize the risk of ecological surprise. Global Change Biology n/a. https://doi.org/10.1111/gcb.15724.

Bergmann, M., Mützel, S., Primpke, S., Tekman, M.B., Trachsel, J., Gerdts, G., 2019. White and wonderful? Microplastics prevail in snow from the Alps to the arctic. Sci. Adv. 5, eaax1157 https://doi.org/10.1126/sciadv.aax1157.

Bianco, A., Sordello, F., Ehn, M., Vione, D., Passananti, M., 2020. Degradation of nanoplastics in the environment: reactivity and impact on atmospheric and surface waters. Sci. Total Environ. 742 (140413) https://doi.org/10.1016/j.scitotenv.2020.140413.

Bigler, M., Svensson, A., Kettner, E., Vallelonga, P., Nielsen, M.E., Steffensen, J.P., 2011. Optimization of high-resolution continuous flow analysis for transient climate signals in ice cores. Environ. Sci. Technol. 45, 4483–4489. https://doi.org/10.1021/es200118j.

Bond, T., Ferrandiz-Mas, V., Felipe-Sotelo, M., Sebille, E. van, 2018. The occurrence and degradation of aquatic plastic litter based on polymer physicochemical properties: a review. Crit. Rev. Environ. Sci. Technol. 48, 685–722. https://doi.org/10.1080/10643389.2018.1483155.

Brahney, J., Hallerud, M., Heim, E., Hahnenberger, M., Sukumaran, S., 2020. Plastic rain in protected areas of the United States. Science 368, 1257–1260. https://doi.org/10.1126/science.aaz5819.

Brahney, J., Mahowald, N., Prank, M., Cornwell, G., Klimont, Z., Matsui, H., Prather, K. A., 2021. Constraining the atmospheric limb of the plastic cycle. Proc. Natl. Acad. Sci. Unit. States Am. 118 https://doi.org/10.1073/pnas.2020719118.

Cai, L., Wang, J., Peng, J., Tan, Z., Zhan, Z., Tan, X., Chen, Q., 2017. Characteristic of microplastics in the atmospheric fallout from Dongguan city, China: preliminary research and first evidence. Environ. Sci. Pollut. Res. 24, 24928–24935. https://doi.org/10.1007/s11356-017-0116-x.

Cappellin, L., Karl, T., Probst, M., Ismailova, O., Winkler, P.M., Soukoulis, C., Aprea, E., Märk, T.D., Gasperi, F., Biasioli, F., 2012. On quantitative determination of volatile organic compound concentrations using proton transfer reaction time-of-flight mass spectrometry. Environ. Sci. Technol. 46, 2283–2290. https://doi.org/10.1021/es203985t.

Carnat, G., Zhou, J., Papakyriakou, T., Delille, B., Goossens, T., Haskell, T., Schoemann, V., Fripiat, F., Rintala, J.-M., Tison, J.-L., 2014. Physical and biological controls on DMS, P dynamics in ice shelf-influenced fast ice during a winter-spring and a spring-summer transitions. J. Geophys. Res.: Oceans 119, 2882–2905. https://doi.org/10.1002/2013JC009381.

Chan, C.K.M., Park, C., Chan, K.M., Mak, D.C.W., Fang, J.K.H., Mitrano, D.M., Chan, C.K. M., Park, C., Chan, K.M., Mak, D.C.W., Fang, J.K.H., Mitrano, D.M., 2021. Microplastic fibre releases from industrial wastewater effluent: a textile wet-processing mill in China. Environ. Chem. 18, 93–100. https://doi.org/10.1071/EN20143.

Cincinelli, A., Scopetani, C., Chelazzi, D., Lombardini, E., Martellini, T., Katsoyiannis, A., Fossi, M.C., Corsolini, S., 2017. Microplastic in the surface waters of the Ross Sea (Antarctica): occurrence, distribution and characterization by FTIR. Chemosphere 175, 391–400. https://doi.org/10.1016/j.chemosphere.2017.02.024.

Davranche, M., Lory, C., Juge, C.L., Blancho, F., Dia, A., Grassl, B., El Hadri, H., Pascal, P.-Y., Gigault, J., 2020. Nanoplastics on the coast exposed to the North atlantic gyre: evidence and traceability. NanoImpact 20 (100262). https://doi.org/10.1016/j.impact.2020.100262.

Dawson, A.L., Kawaguchi, S., King, C.K., Townsend, K.A., King, R., Huston, W.M., Nash, S.M.B., 2018. Turning microplastics into nanoplastics through digestive fragmentation by Antarctic krill. Nat. Commun. 9 (1001) https://doi.org/10.1038/s41467-018-03465-9.

Dris, R., Gasperi, J., Saad, M., Mirande, C., Tassin, B., 2016. Synthetic fibers in atmospheric fallout: a source of microplastics in the environment? Mar. Pollut. Bull. 104, 290–293. https://doi.org/10.1016/j.marpolbul.2016.01.006.

Eicken, H., Lange, M.A., 1989. Development and properties of sea ice in the coastal regime of the southeastern Weddell Sea. J. Geophys. Res.: Oceans 94, 8193–8206. https://doi.org/10.1029/JC094iC06p08193.

El Hadri, H., Gigault, J., Maxit, B., Grassl, B., Reynaud, S., 2020. Nanoplastic from mechanically degraded primary and secondary microplastics for environmental assessments. NanoImpact 17 (100206). https://doi.org/10.1016/j.impact.2019.100206.

Evangeliou, N., Grythe, H., Klimont, Z., Heyes, C., Eckhardt, S., Lopez-Aparicio, S., Stohl, A., 2020. Atmospheric transport is a major pathway of microplastics to remote regions. Nat. Commun. 11 (3381) https://doi.org/10.1038/s41467-020-17201-9.

Ferreira, I., Venâncio, C., Lopes, I., Oliveira, M., 2019. Nanoplastics and marine organisms: what has been studied? Environ. Toxicol. Pharmacol. 67, 1–7. https://doi.org/10.1016/j.etap.2019.01.006.

Geilfus, N.-X., Munson, K.M., Sousa, J., Germanov, Y., Bhugaloo, S., Babb, D., Wang, F., 2019. Distribution and impacts of microplastic incorporation within sea ice. Mar. Pollut. Bull. 145, 463–473. https://doi.org/10.1016/j.marpolbul.2019.06.029.

Geyer, R., Jambeck, J.R., Law, K.L., 2017. Production, use, and fate of all plastics ever made. Sci. Adv. 3 https://doi.org/10.1126/sciadv.1700782.

González-Fernández, D., Cózar, A., Hanke, G., Viejo, J., Morales-Caselles, C., Bakiu, R., Barceló, D., Bessa, F., Bruge, A., Cabrera, M., Castro-Jiménez, J., Constant, M., Crosti, R., Galletti, Y., Kideys, A.E., Machitadze, N., Pereira de Brito, J., Pogojeva, M., Ratola, N., Rigueira, J., Rojo-Nieto, E., Savenko, O., Schöneich-Argent, R.I., Siedlewicz, G., Suaria, G., Tourgeli, M., 2021. Floating macrolitter leaked from Europe into the ocean. Nat. Sustain. 4, 474–483. https://doi.org/10.1038/s41893-021-00722-6.

González-Pleiter, M., Lacerot, G., Edo, C., Pablo Lozoya, J., Leganés, F., Fernández-Piñas, F., Rosal, R., Teixeira-de-Mello, F., 2021. A pilot study about microplastics and mesoplastics in an Antarctic glacier. Cryosphere 15, 2531–2539. https://doi.org/10.5194/tc-15-2531-2021.

Holzinger, R., 2015. PTRwid: a new widget tool for processing PTR-TOF-MS data. Atmos. Meas. Tech 8, 3903–3922. https://doi.org/10.5194/amt-8-3903-2015.

Holzinger, R., Acton, W.J.F., Bloss, W.J., Breitenlechner, M., Crilley, L.R., Dusanter, S., Gonin, M., Gros, V., Keutsch, F.N., Kiendler-Scharr, A., Kramer, L.J., Krechmer, J.E., Languille, B., Locoge, N., Lopez-Hilfiker, F., Materić, D., Moreno, S., Nemitz, E., Quéléver, L.L.J., Sarda Esteve, R., Sauvage, S., Schallhart, S., Sommariva, R., Tillmann, R., Wedel, S., Worton, D.R., Xu, K., Zaytsev, A., 2019. Validity and limitations of simple reaction kinetics to calculate concentrations of organic compounds from ion counts in PTR-MS. Atmos. Meas. Tech. 12, 6193–6208. https://doi.org/10.5194/amt-12-6193-2019.

Hoppmann, M., Richter, M.E., Smith, I.J., Jendersie, S., Langhorne, P.J., Thomas, D.N., Dieckmann, G.S., 2020. Platelet ice, the Southern Ocean's hidden ice: a review. Ann. Glaciol. 61, 341–368. https://doi.org/10.1017/aog.2020.54.

Kelly, A., Lannuzel, D., Rodemann, T., Meiners, K.M., Auman, H.J., 2020. Microplastic contamination in east Antarctic sea ice. Mar. Pollut. Bull. 154 (111130) https://doi.org/10.1016/j.marpolbul.2020.111130.

Kjær, H.A., Vallelonga, P., Svensson, A., Elleskov, L., Kristensen, M., Tibuleac, C., Winstrup, M., Kipfstuhl, S., 2016. An optical dye method for continuous determination of acidity in ice cores. Environ. Sci. Technol. 50, 10485–10493. https://doi.org/10.1021/acs.est.6b00026.

Kjær, H.A., Zens, P., Black, S., Lund, K.H., Svensson, A., Vallelonga, P., 2021a. NEEM to EastGRIP Traverse – spatial variability, seasonality, extreme events and trends in common ice core proxies over the past decades. Clim. Past Discuss. 1–28. https://doi.org/10.5194/cp-2021-99.

Kjær, H.A., Zens, P., Edwards, R., Olesen, M., Mottram, R., Lewis, G., Terkelsen Holme, C., Black, S., Holst Lund, K., Schmidt, M., Dahl-Jensen, D., Vinther, B., Svensson, A., Karlsson, N., Box, J.E., Kipfstuhl, S., Vallelonga, P., 2021b. Recent North Greenland temperature warming and accumulation. Cryosphere Discuss. 1–27. https://doi.org/10.5194/tc-2020-337.

Langway, C.C., 1958. Ice fabrics and the universal stage. This Digital Resource was created from scans of the Print Resource.

Lebreton, L.C.M., van der Zwet, J., Damsteeg, J.-W., Slat, B., Andrady, A., Reisser, J., 2017. River plastic emissions to the world's oceans. Nat. Commun. 8 (15611) https://doi.org/10.1038/ncomms15611.

Legrand, M., McConnell, J., Fischer, H., Wolff, E.W., Preunkert, S., Arienzo, M., Chellman, N., Leuenberger, D., Maselli, O., Place, P., Sigl, M., Schüpbach, S., Flannigan, M., 2016. Boreal fire records in Northern Hemisphere ice cores: a review. Clim. Past 12, 2033–2059. https://doi.org/10.5194/cp-12-2033-2016.

Lehner, R., Weder, C., Petri-Fink, A., Rothen-Rutishauser, B., 2019. Emergence of nanoplastic in the environment and possible impact on human health. Environ. Sci. Technol. 53, 1748–1765. https://doi.org/10.1021/acs.est.8b05512.

Lindeque, P.K., Cole, M., Coppock, R.L., Lewis, C.N., Miller, R.Z., Watts, A.J.R., Wilson-McNeal, A., Wright, S.L., Galloway, T.S., 2020. Are we underestimating microplastic abundance in the marine environment? A comparison of microplastic capture with nets of different mesh-size. Environ. Pollut. 265 (114721) https://doi.org/10.1016/j.envpol.2020.114721.

Lindinger, W., Hansel, A., Jordan, A., 1998. On-line monitoring of volatile organic compounds at pptv levels by means of proton-transfer-reaction mass spectrometry (PTR-MS) medical applications, food control and environmental research. Int. J. Mass Spectrom. Ion Process. 173, 191–241. https://doi.org/10.1016/S0168-1176(97)00281-4.

Liss, P.S., 2020. Microplastics: all up in the air? Mar. Pollut. Bull. 153 (110952) https://doi.org/10.1016/j.marpolbul.2020.110952.

Liu, J., Liang, J., Ding, J., Zhang, G., Zeng, X., Yang, Q., Zhu, B., Gao, W., 2021. Microfiber pollution: an ongoing major environmental issue related to the sustainable development of textile and clothing industry. Environ. Dev. Sustain. 23, 11240–11256. https://doi.org/10.1007/s10668-020-01173-3.

Lorenz, C., Roscher, L., Meyer, M.S., Hildebrandt, L., Prume, J., Löder, M.G.J., Primpke, S., Gerdts, G., 2019. Spatial distribution of microplastics in sediments and surface waters of the southern North Sea. Environ. Pollut. 252, 1719–1729. https://doi.org/10.1016/j.envpol.2019.06.093.

Marina-Montes, C., Pérez-Arribas, L.V., Anzano, J., de Vallejuelo, S.F.-O., Aramendia, J., Gómez-Nubla, L., de Diego, A., Manuel Madariaga, J., Cáceres, J.O., 2022. Characterization of atmospheric aerosols in the antarctic region using Raman spectroscopy and scanning electron microscopy. Spectrochim. Acta Mol. Biomol. Spectrosc. 266 (120452) https://doi.org/10.1016/j.saa.2021.120452.

Masry, M., Rossignol, S., Temime Roussel, B., Bourgogne, D., Bussière, P.-O., R'mili, B., Wong-Wah-Chung, P., 2021. Experimental evidence of plastic particles transfer at the water-air interface through bubble bursting. Environ. Pollut. 280 (116949) https://doi.org/10.1016/j.envpol.2021.116949.

Materić, D., Holzinger, R., Niemann, H., 2021a. Nanoplastics in the Dutch wadden sea (No. EGU21-12012). In: Presented at the EGU21, Copernicus Meetings. https://doi.org/10.5194/egusphere-egu21-12012.

Materić, D., Kasper-Giebl, A., Kau, D., Anten, M., Greilinger, M., Ludewig, E., van Sebille, E., Röckmann, T., Holzinger, R., 2020. Micro- and nanoplastics in alpine snow: a new method for chemical identification and (Semi)Quantification in the nanogram range. Environ. Sci. Technol. 54, 2353–2359. https://doi.org/10.1021/acs.est.9b07540.

Materić, D., Ludewig, E., Brunner, D., Röckmann, T., Holzinger, R., 2021b. Nanoplastics transport to the remote, high-altitude Alps. Environ. Pollut. 117697 https://doi.org/10.1016/j.envpol.2021.117697.

Materić, D., Peacock, M., Dean, J., Futter, M., Maximov, T., Moldan, F., Röckmann, T., Holzinger, R., 2021c. Presence of nanoplastics in rural and remote surface waters. https://doi.org/10.21203/rs.3.rs-548844/v1.

Materić, D., Peacock, M., Kent, M., Cook, S., Gauci, V., Röckmann, T., Holzinger, R., 2017. Characterisation of the semi-volatile component of dissolved organic matter by thermal desorption – proton transfer reaction – mass spectrometry. Sci. Rep. 7 (15936) https://doi.org/10.1038/s41598-017-16256-x.

Morgana, S., Ghigliotti, L., Estévez-Calvar, N., Stifanese, R., Wieckzorek, A., Doyle, T., Christiansen, J.S., Faimali, M., Garaventa, F., 2018. Microplastics in the Arctic: a case study with sub-surface water and fish samples off Northeast Greenland. Environ. Pollut. 242, 1078–1086. https://doi.org/10.1016/j.envpol.2018.08.001.

Napper, I.E., Thompson, R.C., 2019. Environmental deterioration of biodegradable, oxo-biodegradable, compostable, and conventional plastic carrier bags in the sea, soil, and open-air over a 3-year period. Environ. Sci. Technol. 53, 4775–4783. https://doi.org/10.1021/acs.est.8b06984.

Peacock, M., Materić, D., Kothawala, D.N., Holzinger, R., Futter, M.N., 2018. Understanding dissolved organic matter reactivity and composition in lakes and streams using proton-transfer-reaction mass spectrometry (PTR-MS). Environ. Sci. Technol. Lett. 5, 739–744. https://doi.org/10.1021/acs.estlett.8b00529.

Petrich, C., Eicken, H., 2017. Overview of sea ice growth and properties. In: Sea Ice. John Wiley & Sons, Ltd, pp. 1–41. https://doi.org/10.1002/9781118778371.ch1.

PlasticsEurope, 2021. Plastics - the facts 2020.

PlasticsEurope, 2019. Plastics - the facts 2019.

Poulain, M., Mercier, M.J., Brach, L., Martignac, M., Routaboul, C., Perez, E., Desjean, M. C., ter Halle, A., 2019. Small microplastics as a main contributor to plastic mass balance in the North atlantic subtropical gyre. Environ. Sci. Technol. 53, 1157–1164. https://doi.org/10.1021/acs.est.8b05458.

Revell, L.E., Kuma, P., Le Ru, E.C., Somerville, W.R.C., Gaw, S., 2021. Direct radiative effects of airborne microplastics. Nature 598, 462–467. https://doi.org/10.1038/s41586-021-03864-x.

Rezaei, M., Riksen, M.J.P.M., Sirjani, E., Sameni, A., Geissen, V., 2019. Wind erosion as a driver for transport of light density microplastics. Sci. Total Environ. 669, 273–281. https://doi.org/10.1016/j.scitotenv.2019.02.382.

Ross, P.S., Chastain, S., Vassilenko, E., Etemadifar, A., Zimmermann, S., Quesnel, S.-A., Eert, J., Solomon, E., Patankar, S., Posacka, A.M., Williams, B., 2021. Pervasive distribution of polyester fibres in the Arctic Ocean is driven by Atlantic inputs. Nat. Commun. 12 (106) https://doi.org/10.1038/s41467-020-20347-1.

Rowlands, E., Galloway, T., Manno, C., 2021. A Polar outlook: potential interactions of micro- and nano-plastic with other anthropogenic stressors. Sci. Total Environ. 754 (142379) https://doi.org/10.1016/j.scitotenv.2020.142379.

Schüpbach, S., Fischer, H., Bigler, M., Erhardt, T., Gfeller, G., Leuenberger, D., Mini, O., Mulvaney, R., Abram, N.J., Fleet, L., Frey, M.M., Thomas, E., Svensson, A., Dahl-Jensen, D., Kettner, E., Kjaer, H., Seierstad, I., Steffensen, J.P., Rasmussen, S.O., Vallelonga, P., Winstrup, M., Wegner, A., Twarloh, B., Wolff, K., Schmidt, K., Goto-Azuma, K., Kuramoto, T., Hirabayashi, M., Uetake, J., Zheng, J., Bourgeois, J., Fisher, D., Zhiheng, D., Xiao, C., Legrand, M., Spolaor, A., Gabrieli, J., Barbante, C., Kang, J.-H., Hur, S.D., Hong, S.B., Hwang, H.J., Hong, S., Hansson, M., Iizuka, Y., Oyabu, I., Muscheler, R., Adolphi, F., Maselli, O., McConnell, J., Wolff, E.W., 2018. Greenland records of aerosol source and atmospheric lifetime changes from the Eemian to the Holocene. Nat. Commun. 9 (1476) https://doi.org/10.1038/s41467-018-03924-3.

Sullivan, G.L., Gallardo, J.D., Jones, E.W., Hollliman, P.J., Watson, T.M., Sarp, S., 2020. Detection of trace sub-micron (nano) plastics in water samples using pyrolysis-gas chromatography time of flight mass spectrometry (PY-GCToF). Chemosphere 249 (126179). https://doi.org/10.1016/j.chemosphere.2020.126179.

Tagg, A.S., Brandes, E., Fischer, F., Fischer, D., Brandt, J., Labrenz, M., 2021. Agricultural application of microplastic-rich sewage sludge leads to further uncontrolled contamination. Sci. Total Environ. 150611 https://doi.org/10.1016/j.scitotenv.2021.150611.

Tison, J.-L., Lorrain, R.D., Bouzette, A., Dini, M., Bondesan, A., StiéVenard, M., 1998. Linking landfast sea ice variability to marine ice accretion at hells gate ice shelf, Ross Sea, in: Antarctic sea ice: physical processes, interactions and variability. American Geophysical Union (AGU) 375–407. https://doi.org/10.1029/AR074p0375.

Van der Linden, F.C., Tison, J.-L., Champenois, W., Moreau, S., Carnat, G., Kotovitch, M., Fripiat, F., Deman, F., Roukaerts, A., Dehairs, F., Wauthy, S., Lourenço, A., Vivier, F., Haskell, T., Delille, B., 2020. sea ice CO2 dynamics across seasons: impact of processes at the interfaces. J. Geophys. Res.: Oceans 125. https://doi.org/10.1029/2019JC015807 e2019JC015807.

Vicente, J.S., Gejo, J.L., Rothenbacher, S., Sarojiniamma, S., Gogritchiani, E., Wörner, M., Kasper, G., Braun, A.M., 2009. Oxidation of polystyrene aerosols by VUV-photolysis and/or ozone. Photochem. Photobiol. Sci. 8, 944–952. https://doi.org/10.1039/B902749A.

Wahl, A., Le Juge, C., Davranche, M., El Hadri, H., Grassl, B., Reynaud, S., Gigault, J., 2021. Nanoplastic occurrence in a soil amended with plastic debris. Chemosphere 262 (127784). https://doi.org/10.1016/j.chemosphere.2020.127784.

Wayman, C., Niemann, H., 2021. The fate of plastic in the ocean environment – a minireview. Environ. Sci.: Processes Impacts. https://doi.org/10.1039/D0EM00446D.

Weiss, L., Ludwig, W., Heussner, S., Canals, M., Ghiglione, J.-F., Estournel, C., Constant, M., Kerhervé, P., 2021. The missing ocean plastic sink: gone with the rivers. Science 373, 107–111. https://doi.org/10.1126/science.abe0290.

Xu, G., Cheng, H., Jones, R., Feng, Y., Gong, K., Li, K., Fang, X., Tahir, M.A., Valev, V.K., Zhang, L., 2020. Surface-enhanced Raman spectroscopy facilitates the detection of microplastics <1 μm in the environment. Environ. Sci. Technol. 54, 15594–15603. https://doi.org/10.1021/acs.est.0c02317.

Zhang, Y., Gao, T., Kang, S., Allen, S., Luo, X., Allen, D., 2021. Microplastics in glaciers of the Tibetan Plateau: evidence for the long-range transport of microplastics. Sci. Total Environ. 758 (143634) https://doi.org/10.1016/j.scitotenv.2020.143634.

Zhu, X., Huang, W., Fang, M., Liao, Z., Wang, Y., Xu, L., Mu, Q., Shi, C., Lu, C., Deng, H., Dahlgren, R., Shang, X., 2021. Airborne microplastic concentrations in five megacities of northern and southeast China. Environ. Sci. Technol. 55, 12871–12881. https://doi.org/10.1021/acs.est.1c03618.